Microchemical Journal 137 (2018) 342–347

Contents lists available at ScienceDirect

Microchemical Journal

journal homepage: www.elsevier.com/locate/microc

Evaluation of time-gated Raman spectroscopy for the determination of nitric, sulfuric and hydrofluoric acid concentrations in pickle liquor

Bryan Heilala [a,c], Ari Mäkinen [a], Ilkka Nissinen [b], Jan Nissinen [b], Anssi Mäkynen [a], Paavo Perämäki [c,*]

[a] Optoelectronics and Measurement Techniques, University of Oulu, P.O Box 8000, 90014 Oulu, Finland
[b] Circuits and systems, University of Oulu, P.O Box 8000, 90014 Oulu, Finland
[c] Research Unit of Sustainable Chemistry, University of Oulu, P.O Box 3000, 90014 Oulu, Finland

ARTICLE INFO

Article history:
Received 11 July 2017
Received in revised form 15 November 2017
Accepted 17 November 2017
Available online 20 November 2017

Keywords:
Raman spectroscopy
Time-gated
Pickle liquor
Acid
Quantification

ABSTRACT

The focus of this study was to assess the feasibility of time-gated Raman spectroscopy for stainless steel pickle liquor acid quantification. Pickle liquor is used for dissolving metal surface impurities during the pickling process. The pickle liquor samples consisted mainly of 11–89 g/L HNO_3, 20–160 g/L H_2SO_4, 5–57 g/L HF and stainless steel residue. Raman peaks correlating with the different acids were identified in both aqueous and pickle liquor solutions. The linearity between Raman scattering intensity and acid concentration was studied. Multivariate PLSR calibration for pickle liquor HNO_3, H_2SO_4 and HF quantification was also investigated. Time-gated Raman spectroscopy was found to be a promising technique for pickle liquor HNO_3 and H_2SO_4 quantification.

1. Introduction

In the field of metal industry, various surface treatments often require that rust and other surface impurities are removed. During the pickling process some of the metal surface dissolves in the corrosive pickling liquor removing the surface impurities in the process [1,2]. Pickle liquors can be divided into two groups: Liquors used in galvanizing plants and liquors used in stainless steel rolling mills. Galvanizing plant pickling liquors usually consist primarily of hydrochloric acid and metal ions. The pickle liquors in steel rolling mills are usually more complex acid mixtures and they contain primarily hydrofluoric and nitric or sulfuric acid and metal ions [1]. Pickle liquor samples used in this study also contained sulfuric acid in addition to hydrofluoric and nitric acid.

Acid contents of pickle liquors have to be known in order to achieve the best pickling results. Methods used for pickling bath acid concentration measurements include acid-base titrations for total and free acid concentration determination and the use of fluoride selective electrode for hydrofluoric acid concentration determination [2,3]. Also multisensor techniques have been developed that make use of combined analysis methods including ion selective electrode, ultrasonic speed, conductivity, density and refraction index measurements [4,5].

This study was aimed at assessing the suitability of Raman spectroscopy for one-step acid analysis of stainless steel pickling bath process liquors. The method could be used to save on acid consumption and to reduce chemical metal surface wear. Raman spectroscopy is a convenient analysis technique that requires minimal sample preparation and enables on-line measurements. Raman spectroscopy is also suited for analysis of aqueous samples unlike many techniques based on IR spectroscopy. The currently used pickle liquor analysis methods are quite time consuming. Developing a continuous analysis method would provide valuable information about the pickling bath composition in shorter time intervals and it would also enable faster adjustment of pickle liquor composition.

Measurements in this study were done using a time-gated Raman spectrometer. Fluorescence emission from the sample solution has a longer delay compared with Raman scattering, which is almost instantaneous. A time-gated Raman apparatus exploits this time difference and is capable of fluorescence rejection. Time-gated Raman techniques are usually used for samples with disruptive levels of fluorescence. In this study, the analyzed sample solutions exhibited a low amount of fluorescence except for fluorescence originating from the plastic cuvettes. However, time gating usually keeps the spectra background quite low and makes the measurements less susceptible to stray light and cosmic rays, which in turn reduces the need for preprocessing of the spectral data. Earlier research focusing on quantification of three different pickling bath mineral acids using time-gated Raman spectroscopy has not been published to the best of the authors knowledge.

* Corresponding author.
E-mail address: paavo.peramaki@oulu.fi (P. Perämäki).

https://doi.org/10.1016/j.microc.2017.11.010
0026-265X/

2. Experimental

2.1. Reagents

The following analysis grade acids (Merck Millipore) were used in this study: 65% HNO_3, 95–97% H_2SO_4, and 40% HF. The water used for sample preparation and cuvette rinsing was purified with a Merck Millipore Elix system.

2.2. Sample solution and reference measurements

The pickle liquor samples used in this study consisted of 11–89 g/L HNO_3, 20–160 g/L H_2SO_4, 5–57 g/L HF, and 6–59 g/L iron. Because the pickle liquors were used for stainless steel pickling, they probably contained several other metals in addition to iron.

At the stainless steel factory where the pickle liquor samples were received from, the total acid concentrations were determined with NaOH titration and SO_4^{2-} concentrations were measured using nephelometry with a $BaSO_4$ precipitate. Fluoride and nitrate concentrations were measured using ion selective electrodes. The pickle liquor acid concentrations are calculated using the measurement results of the aforementioned analysis methods. In this study, these measurement results were used as reference results. The quality control measurements for these reference analysis techniques are conducted using aqueous acid samples without the actual pickle liquor sample matrix. The QC measurements of a time period of about 18 months ($n = 70$) had a standard deviation of 0.85 g/L for HNO_3 (31.5 g/L concentration), 2.8 g/L for H_2SO_4 (98.0 g/L concentration) and 0.49 g/L for HF (10 g/L concentration).

2.3. Instrumentation

Raman measurements were done with a time-gated experimental Raman spectrometer equipped with a single photon avalanche diode (SPAD) detector [6–8]. An experimental 532 nm pulsed laser was used for sample illumination. The pulsed micro-chip laser was based on a semiconductor saturable absorber mirror (SESAM) having a pulse width (full width at half maximum) and energy of approximately 150 ps and 0.2 μJ, respectively.

Before the determinations utilizing multivariate data analysis in calibration, the Raman spectrometer was upgraded with a new laser that enabled shorter measurement times. It was verified that no spectra drift or changes caused by sample heating were present while using the more powerful laser. The new Teem Photonics 532 nm laser had a repetition rate of 360 kHz, $\Delta\lambda$ of <0.11 nm, pulse width (FWHM) of 160 ps and pulse energy of 1 μJ resulting to approximately 300 mW of average power.

Initial measurements without HF were done using glass cuvettes and the later measurements with samples containing HF were done using disposable plastic BRAND UV cuvettes (BRAND GMBH + CO KG; Wertheim, Germany). The plastic cuvettes produced several Raman peaks but they were removed using blank correction. Data collection time was about 5 min per sample with the first laser and about 3 min with the Teem Photonics laser. Data processing, peak fitting and peak area integration were done using an in-house script in the MATLAB R2016b software environment (The MathWorks, Massachussetts). Unscrambler 10.4.1 software package (CAMO Software AS, Norway) was used for multivariate data analysis.

3. Results and discussion

3.1. Spectra

Peaks due to HNO_3 and H_2SO_4 were first identified from aqueous solutions with various acid concentrations (Fig. 1). The identified peaks were at the 1100–300 cm^{-1} wavenumber region. Sulfuric acid

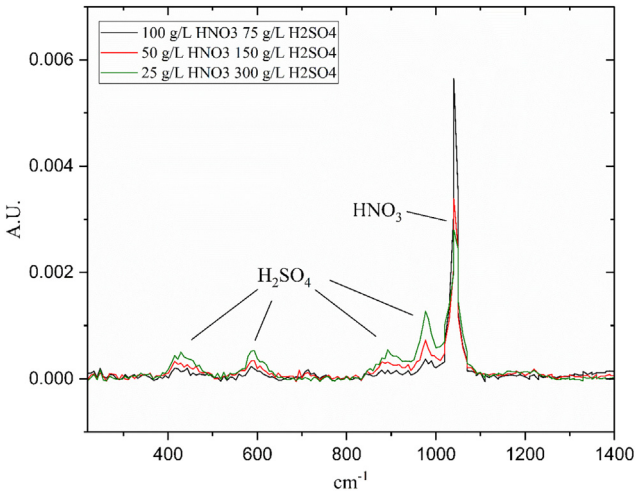

Fig. 1. Raman peaks due to aqueous solutions of H_2SO_4 (75, 150 and 300 g/L) and HNO_3 (100, 50 and 25 g/L).

produced several peaks (977, 892, 592 and 429 cm^{-1}). The peaks at 429 and 592 cm^{-1} can probably be assigned to bisulfate ion, 892 cm^{-1} peak to HSO_4^- symmetric stretch (ν_1) and 977 cm^{-1} to SO_4^{2-} bend (ν_2) [9,10]. Nitric acid produced one identified peak (1042 cm^{-1}). This peak corresponds to nitrate ion symmetric stretch band [11]. These findings are in agreement with previous reports [9–12].

Linear dependence between the intensity of Raman scattering and concentration was observed for both HNO_3 and H_2SO_4. Although the responses seemed linear even when analyzing solutions containing both HNO_3 and H_2SO_4, sulfuric acid produces some Raman scattering (HSO_4^- (ν_3) and (ν_4) modes) at the HNO_3 1042 cm^{-1} wavenumber region [9,10,12,13]. Hence a multivariate model might be a more suitable data analysis method in part because of this (discussed more in depth later).

Any Raman peaks correlating with sample HF concentration were not observed with the time-gated Raman spectrometer used. In addition to the 1870–220 cm^{-1} wavenumber range, the 3520–1870 cm^{-1} range was also scanned to check for any relevant Raman peaks. No usable peaks due to HF were detected in aqueous samples even when measuring samples with high HF concentrations of 110–225 g/L. However, Raman signals due to HF have been reported earlier although with a different Raman apparatus and laser wavelength [11].

An earlier paper [14] suggests that Raman peaks due to HF might be difficult to observe in a sample matrix containing sulfuric acid. Sulfuric acid might react with hydrofluoric acid producing fluorosulfonic acid dampening the HF Raman peaks. The researchers were able to correlate fluorosulfonic acid peaks (1082 and 810 cm^{-1}) with HF concentrations. In this study however, no quantifiable peaks due to $HFSO_3$ were observed. Neither were any changes observed in H_2SO_4 peaks with varying HF concentrations.

The features of the spectra originating from pickle liquor samples (Figs. 2 and 3) were not significantly different from the aqueous solution spectra. The pickle liquor matrix produced some additional noise and a minor peak between the 592 and 429 cm^{-1} sulfuric acid peaks. No shifts in HNO_3 or H_2SO_4 peak positions were observed. However, high iron concentrations may affect sulfate band positions [13].

Even though the pickle liquor pH was quite low, a dark blue precipitate was observed at the bottom of the cuvettes when the pickle solution was kept in the cuvettes for several days. Precipitation could affect the measurements and it would probably be desirable to analyze the samples shortly after sampling. This was not, however, possible during this study.

The measured Raman peak intensities were lower in pickle liquor spectra compared with aqueous sample spectra. The pickle liquor

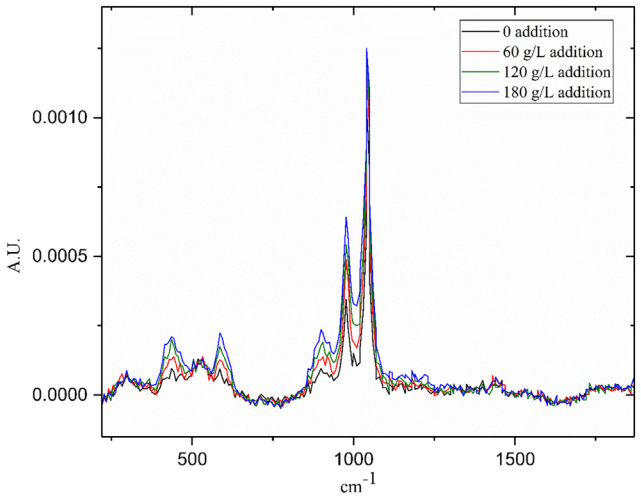

Fig. 2. Raman peaks in the pickle liquor after additions of H_2SO_4 (0, 60, 120 and 180 g/L additions).

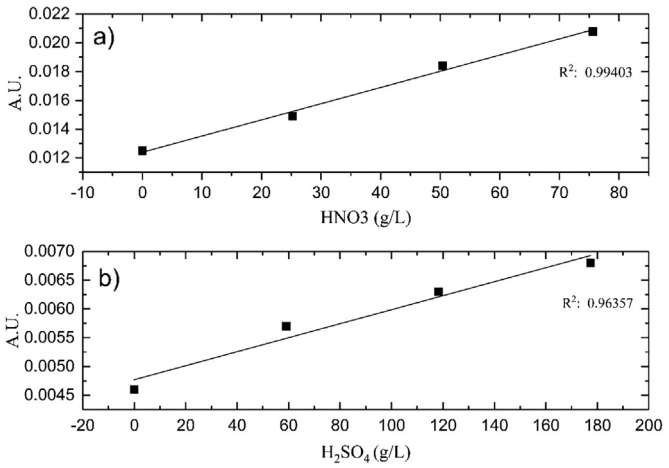

Fig. 4. The intensity of Raman scattering for pickle liquor solutions where varying concentrations of a) HNO_3 (1042 cm^{-1} Raman peak) and b) H_2SO_4 (977 cm^{-1} Raman peak) were added. The X-axes indicate the concentrations of acid additions.

matrix had a dark blue color and the matrix absorption was suspected to be greater than in aqueous solutions. Because of this, external calibration using aqueous solutions would not be directly applicable for pickle liquor acid quantification.

3.2. Univariate calibration

The intensity (peak areas) of the 1042 and 977 cm^{-1} Raman peaks seemed to increase quite linearly when known amounts of HNO_3 and H_2SO_4 were added to real pickling solutions (Fig. 4). Thus, the standard addition method was considered for HNO_3 and H_2SO_4 quantification.

In some cases, standard addition method may be used as a calibration method to compensate the observed matrix effects, e.g. signal attenuation in a real sample matrix. However, even though the Raman scattering intensity seemed to increase linearly with the additions in most cases, the standard addition method was not successful in this case and the calculated HNO_3 and H_2SO_4 concentrations were too high compared with the reference results. An unknown background enhancement was speculated to be the reason for the difficulties in using the standard addition method. Due to these aforementioned difficulties, the use of the standard addition method for pickle liquor acid quantification was not investigated further.

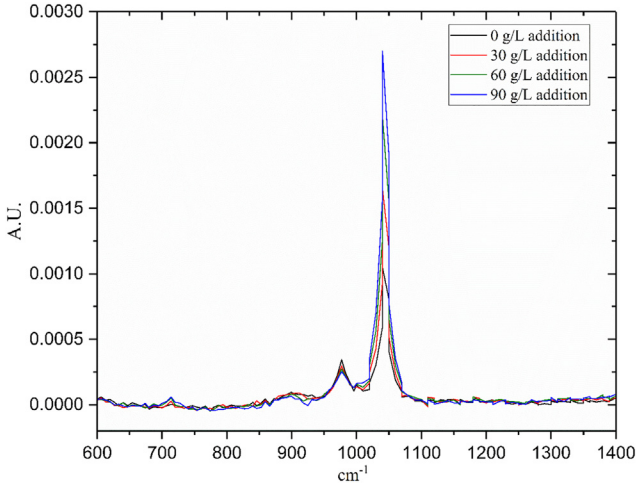

Fig. 3. Raman peaks in the pickle liquor after additions of HNO_3 (0, 30, 60 and 90 g/L additions).

Calibration curves were also constructed using unmodified and undiluted pickle liquor samples as calibration standards. When using the reference results (reference methods are presented in the experimental section) for calibration, it has to be noted that uncertainty of the reference results will increase the uncertainty of the calibration model. The 1042 and 977 cm^{-1} peak areas were used for HNO_3 and H_2SO_4 calibration curves. The peak area determination and calibration testing was done with and without pseudo Voigt peak fitting (in-house MATLAB script) that varies the fitted line shape using linear combination of Gaussian and Lorentzian peak shapes. The goal of using the peak fitting was to resolve some of the peak overlapping. In practice, the effect of the peak fitting on the calibration curve was quite minor. The calibration curves that were constructed using the undiluted pickle liquors were clearly ascending curves but the deviation of the calibration points was quite high and the R-squared values for the linear fittings were quite low (Figs. 5 and 6). The peak intensities (peak areas) for Figs. 5 and 6 were calculated without peak fitting. The integration limits for the peaks were 1003–957 cm^{-1} (H_2SO_4) and 1080–1009 cm^{-1} (HNO_3). The measurement results used for the univariate calibration were collected during a single measurement run (a single spectrum with $30 * 10^6$ laser pulses which amounts to about a 3 min acquisition time per sample). The same measurement data was also used for multivariate data manipulation.

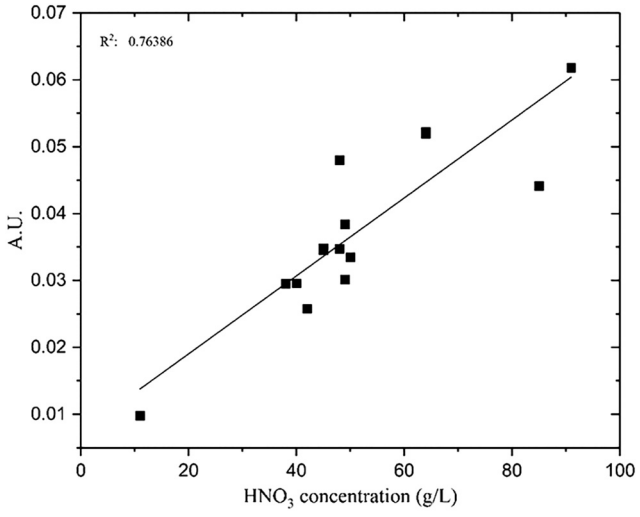

Fig. 5. Linear calibration fitting for HNO_3 constructed using undiluted pickle liquor samples.

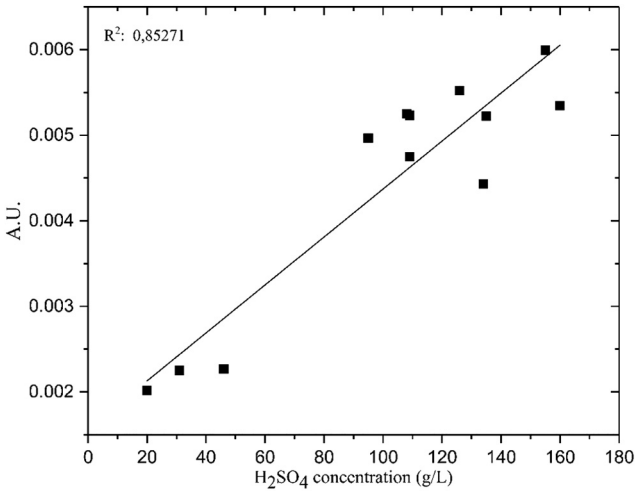

Fig. 6. Linear calibration fitting for H_2SO_4 constructed using undiluted pickle liquor samples.

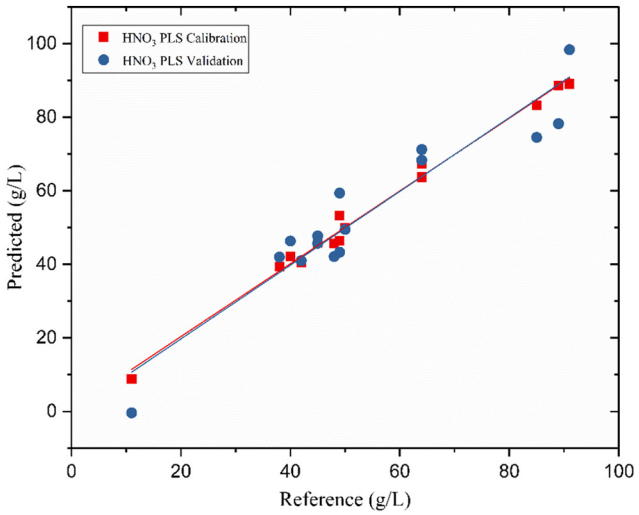

Fig. 7. HNO_3 PLSR calibration (RMSEC: 2.06669042, R^2: 0.9900864) and cross validation (RMSECV: 6,9294014, R^2: 0,9029367) plot.

3.3. Multivariate calibration

Multivariate calibration methods are widely used in Raman and IR spectroscopy [15,16]. A PLSR (Partial Least Squares Regression) model was applied for the HF, HNO_3 and H_2SO_4 concentration determination using the Unscrambler 10 data analysis software and its NIPALS algorithm. Multivariate calibration methods take into account partial peak overlapping and the correlation of several peaks. It was also investigated, if the multivariate chemometric method would reveal any correlation between the Raman spectra and the reference HF concentrations.

15 pickle liquor samples were available for the formation of the PLSR calibration model. For three of the samples no reference H_2SO_4 measurement results were available and so only 12 samples were used for the H_2SO_4 PLSR model. HNO_3 and HF reference results were available for every sample. All of the measurement data used for the multivariate analysis was collected during the same measurement run.

The spectra used for the PLSR models were blank (cuvette) corrected. No other spectral data preprocessing was used. Time-gated Raman measurements are less susceptible to stray light and cosmic rays. Because of this, in most cases time-gating completely eliminates the need for cosmic ray removal in the spectral preprocessing step. Both multiplicative scatter correction (more often used in IR spectroscopy [15]) and Savitzky-Golay smoothing (second order, 5 point (32.2 cm^{-1}) moving windows), were tested as preprocessing options but neither of these methods produced improved prediction results.

The first PLSR models were constructed using all of the sample measurement data because of the limited amount of available samples. A full leave one out cross validation (LOOCV) setup was used for the model validation. Both root mean square error (RMSE) and R-squared values of the cross validation and calibration plots were used for the model evaluation (Figs. 7 and 8). The amount of factors used for the models were chosen using the RMSE values, explained variance and residual variance for different numbers of factors. The Unscrambler software also suggests the optimal amount of factors and these suggestions were in agreement with the number of chosen factors (HNO_3: 5 factors, H_2SO_4: 3 factors).

The PLSR calibration and validation prediction results are presented in Table 1. The LOOCV validation prediction results are a more realistic approximation of prediction capabilities of the PLSR model. The sample concentration distribution should also be considered. For example, there was only one sample in the available sample group with a low (11 g/L) HNO_3 concentration so the low HNO_3 concentration predictions were probably less accurate (sample 11 in Table 1).

3.4. Comparison of univariate and multivariate calibration

The univariate least squares linear regression models (Figs. 5 and 6) were also treated with a LOOCV type procedure. One measurement result at a time was moved from the calibration set to the prediction set and using the univariate least squares linear regression the concentration of each prediction set was predicted (Table 1).

The PLSR validation prediction results are closer to the reference measurement results than the univariate least squares validation prediction results. This indicates that PLSR might be a better calibration model than the univariate linear least squares model for pickle liquor HNO_3 and H_2SO_4 quantification. The reliability of the PLSR model can be evaluated thoroughly in the future when more analytical data and samples are available.

A more thorough comparison of these two calibration methods also requires comparison and evaluation of uncertainties and confidence intervals. Rough estimations of PLSR prediction uncertainties can be made using prediction and cross validation RMSE values. However, attaching one single standard error to all predictions is less than optimal. The RMSECV value is 6,9 for the HNO_3 and 10,0 for the H_2SO_4 PLSR model with the leave one out cross validation.

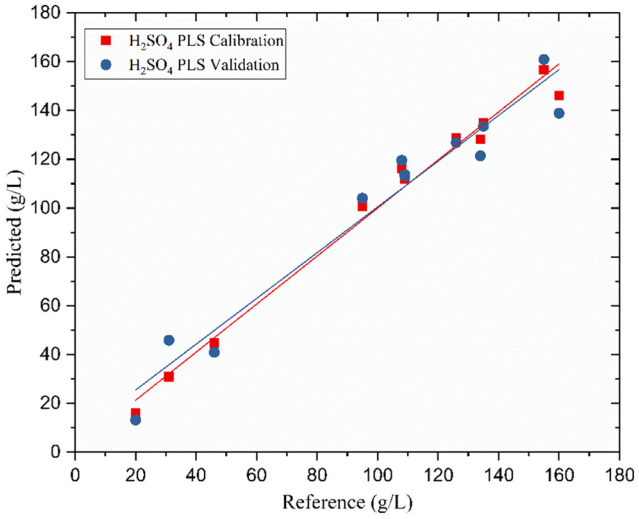

Fig. 8. H_2SO_4 PLSR calibration (RMSEC: 5,6121264, R^2: 0.9842156) and cross validation (RMSECV: 9,9697256, R^2: 0.9581436) plot.

Table 1
PLSR calibration and cross validation prediction results, univariate least square linear regression validation results and reference measurement results for HNO_3 and H_2SO_4 concentrations.

HNO_3 [g/L]	Reference value	PLSR calib.	PLSR valid.	Univariate[a] valid.	H_2SO_4 [g/L]	Reference value	PLSR calib.	PLSR valid.	Univariate[a] valid.
Sample 1	64	63.7	68.3	83.7	Sample 1	20	16.1	13.2	13.4
Sample 2	49	53.2	59.4	40.0	Sample 2	31	30.9	45.9	21.3
Sample 3	40	42.1	46.3	39.6	Sample 3	108	116.3	119.6	133.6
Sample 4	42	40.4	41.0	31.4	Sample 4	134	128.2	121.4	99.2
Sample 5	50	49.9	49.5	46.7	Sample 5	126	128.8	126.9	143.0
Sample 6	38	39.4	42.0	46.7	Sample 6	109	112.0	113.2	113.9
Sample 7	45	46.3	47.7	39.7	Sample 7	109	112.4	113.7	132.9
Sample 8	91	89.0	98.4	104.4	Sample 8	46	44.7	40.9	17.3
Sample 9	64	67.3	71.2	84.3	Sample 9	95	100.8	104.0	123.5
Sample 10	49	46.4	43.3	56.7	Sample 10	155	156.7	160.9	158.5
Sample 11	11	8.8	−0.4	−3.3	Sample 12	135	134.9	133.5	129.7
Sample 12	45	45.9	45.7	49.2	Sample 14	160	146.1	138.9	130.0
Sample 13	85	83.2	74.5	64.2					
Sample 14	48	45.7	42.1	49.3					
Sample 15	89	88.6	78.2	71.0					

[a] Univariate least squares linear regression LOOCV type validation

The Unscrambler program can be used to calculate deviations for the PLSR predictions. Earlier unscrambler deviation calculation methods have been criticized [17,18] but the calculation method has been improved for newer unscrambler program versions [19]. The deviation estimation method is outlined in Unscrambler method references document [19] and the deviation estimates for each LOOCV acid concentration prediction are presented in Table 2. Uncertainty estimation for multivariate calibration is discussed in more detail elsewhere [20,21].

Standard deviations of a least squares prediction (x_0) can be approximated using the least squares regression line information in combination with Eq. (1) [22]:

$$s_{x_0} = \frac{s_y/_x}{b}\sqrt{1+\frac{1}{n}+\frac{(y_0-y\sim)^2}{b^2\sum_i (x_i-x\sim)^2}} \quad (1)$$

where S_{x0} is the estimated standard deviation of x_0, $S_{y/x}$ is the uncertainty of regression, b is the slope of the regression line, n is the amount of observations used for the regression line, y_0 is the experimental value of y from which the concentration value x_0 is to be determined. Rest of the variables are x and y values or mean x and y values used in the regression line.

The calculated S_{xo} values for each leave one out least squares sample are presented in Table 2. The calculated PLSR deviations are smaller than the calculated univariate deviations. Comparing multivariate and univariate deviations and uncertainties is not a simple or an unambiguous process especially with a very limited data set.

3.5. Further PLSR model testing

After constructing the PLSR models using all of the available sample data, measurement data of three samples with varying acid concentrations were separated from the calibration set and used as a prediction set (prediction results are presented in Table 3). The new H_2SO_4 calibration PLSR model was constructed using measurement data of 9 samples. Using only a few spectra for PLSR model formation will in most cases deteriorate the prediction capabilities of the model. As expected, the PLSR models constructed with a smaller calibration sample set resulted in lowered model validation RMSE and R-squared values. The prediction results of the three samples (Table 3) are slightly further off the reference results than the first PLSR validation results (Table 1) with all of the sample measurement data used as a calibration set. A proper model evaluation and validation would require more thorough testing with a more extensive test set [23].

For testing purposes 840–767 cm^{-1} and 1870–1499 cm^{-1} wavenumber regions were removed from the Raman spectra of every pickle liquor sample and the HNO_3 and H_2SO_4 PLSR models were constructed again with the reduced spectra. The removed wavenumber areas were evaluated beforehand to contain no relevant spectral information. The reduced PLSR models and their validation results were very similar or in some cases almost identical to the earlier PLSR models that were constructed using full spectra. This indicates that the noise in the "empty" spectral areas does not significantly affect the reliability of the PLSR models.

The HF PLSR model could not find any clear correlation between the spectral data and HF concentrations (Fig. 9) which is in line with the

Table 2
Deviation values for the PLSR and univariate least squares predictions.

HNO_3	PLSR deviation	Univariate deviation	H_2SO_4	PLSR deviation	Univariate deviation
Sample 1	8.9	12.5	Sample 1	20.2	28.1
Sample 2	5.6	11.8	Sample 2	19.3	26.9
Sample 3	4.6	12.2	Sample 3	6.5	21.3
Sample 4	4.7	12.2	Sample 4	9.1	18.1
Sample 5	4.5	11.9	Sample 5	12.0	22.8
Sample 6	4.4	12.2	Sample 6	6.5	22.4
Sample 7	5.5	11.9	Sample 7	8.2	21.5
Sample 8	5.3	15.4	Sample 8	26.2	25.9
Sample 9	5.3	12.5	Sample 9	7.5	20.2
Sample 10	5.1	11.8	Sample 10	12.5	24.3
Sample 11	5.6	17.3	Sample 12	6.7	22.6
Sample 12	5.1	11.9	Sample 14	5.6	19.1
Sample 13	6.1	15.4			
Sample 14	5.0	12.0			
Sample 15	6.5	10.0			

Table 3
Prediction results of three sample measurement results that were moved from the original PLSR calibration set to the PLSR prediction set and the calculated deviation of the PLSR prediction.

HNO_3	Reference value [g/L]	Predicted [g/L]	Deviation [g/L]	H_2SO_4	Reference value [g/L]	Predicted [g/L]	Deviation [g/L]
Sample 1	64	68,9	7,8	Sample 2	31	46,9	14,4
Sample 6	38	43,9	5,1	Sample 9	95	98	8,6
Sample 13	85	73,6	6,4	Sample 10	155	161,8	8,2

lack of observations of Raman peaks originating from HF during this study. If the direct measurement of HF cannot be achieved with the experimental setup used in this study, a fluoride selective electrode [2,3,24] could potentially be used in conjunction with the Raman apparatus to quantify all three acids. However, continuous fluoride selective electrode measurements might not be feasible because of electrode material corrosion [5].

The PLSR calibration results seem quite promising for HNO_3 and H_2SO_4 quantification even when using a limited amount of samples and measurement data. Once again, it has to be noted that when using reference results for calibration, the uncertainty of the reference measurements also increases the uncertainty of the calibration model. The validity assessment and updating [25,26] of the calibration model during longer measurement periods and in industrial conditions requires further studies.

4. Conclusions

Time-gated Raman spectroscopy can be used for HNO_3 and H_2SO_4 pickle liquor quantification utilizing a multivariate calibration model. Several Raman peaks due to HNO_3 (1042 cm^{-1}) and H_2SO_4 (977, 892, 592 and 429 cm^{-1}) were identified and the peak areas seem to correlate quite linearly with the acid concentrations. The Raman peaks were observable in both aqueous and pickle liquor samples. PLSR calibration model prediction results were more in line with the reference results than prediction results calculated using a more traditional univariate linear calibration model. The results obtained in this study are promising and it is expected, that time gated Raman spectroscopy can be utilized as a simple and rapid tool for the determination of HNO_3 and H_2SO_4 concentrations in pickle liquor. However, no Raman peaks correlating with HF concentrations were observed using the time-gated Raman spectrometer.

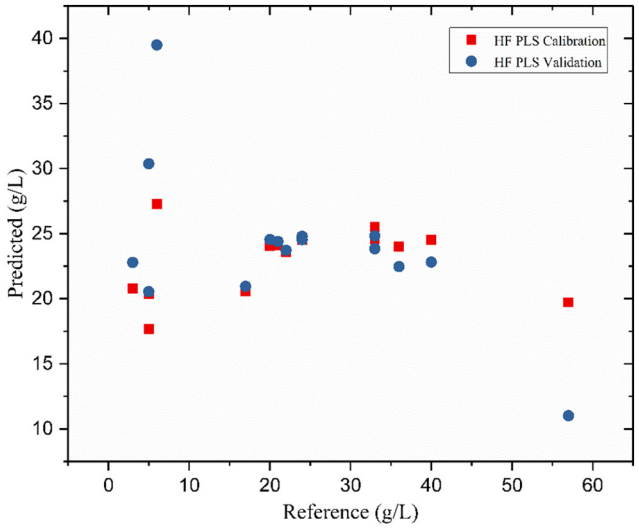

Fig. 9. HF PLSR calibration (RMSE: 14.39366, R^2: 0.0297452) and validation (RMSE: 18.60931, R^2: NA) plot.

Acknowledgments

We would like to thank Dr. Leeni Aula and Johanna Ikäheimonen at Outokumpu Stainless Ltd. for providing the pickle liquor samples and information related to the samples. We would also like to thank Jussi Tenhunen at VTT Ltd. for letting us use their continuous wave Raman spectrometer. Many thanks to everyone at TimeGate Instruments Ltd. as well for letting us use their time-gated Raman spectrometer.

Conflict of interest

Bryan Heilala is affiliated with a company that produces time-gated Raman instruments that are based on CMOS SPAD detectors.

References

[1] A. Devi, A. Singhal, R. Gupta, P. Pansade, Clean Techn. Environ. Policy 16 (2014) 1515.
[2] K. Lindroos, Analyst 112 (1987) 71.
[3] T. Eriksson, Anal. Chim. Acta 65 (1973) 417.
[4] Rodabaugh, R. D.; Price, D. M.; Bryant, G. A.; United States patent US 20020146348, 2002.
[5] M. Werner, R. Wolters, H.-G. Hartmann, D. Buchloh, M.J.G. Bonany, D.F. Rengel, M. Böch-Schnepps, F. Quirgs, T. Blomfeldt, K. Jackobson, EU Research KI-NA-26906-EN-N (Flexpromus), 2014.
[6] I. Nissinen, J. Nissinen, A. Länsman, L. Hallman, A. Kilpelä, J. Kostamovaara, M. Kögler, M. Aikio, J. Tenhunen, J. Proc. of ESSDERC'11, vol. 12–16, 2011 375.
[7] I. Nissinen, J. Nissinen, P. Keränen, A. Länsman, J. Holma, J. Kostamovaara, IEEE J. Sens. 15 (2015) 1358.
[8] J. Kostamovaara, J. Tenhunen, M. Kögler, I. Nissinen, J. Nissinen, P. Keränen, Opt. Express 21 (2013), 31632. .
[9] G.E. Walrafen, W.H. Yang, Y.C. Chu, J. Phys. Chem. 106 (2002), 10162. .
[10] R.H. Hunt, A.D. Ward, M.D. King, RSC Adv. 3 (2013), 19448. .
[11] G. Kang, K. Lee, H. Park, J. Lee, Y. Jung, K. Kim, B. Son, H. Park, Talanta 81 (2010) 1413.
[12] R.A. Cox, U.L. Haldna, L.K. Idler, K. Yates, Can. J. Chem. 59 (1981) 2591.
[13] F. Sobron, P. Sobron, F. Rull, A. Sanz, J. Medina, C.J. Nielsen, Spectrochim. Acta A Mol. Biomol. Spectrosc. 68 (2007) 1138.
[14] D.C. Ford, C. Cooper, L.D. Cooley, C. Thompson, D. Bouchard, B. Albee, S. Bishnoi, J. Electrochem. Soc. 160 (2013) H398.
[15] R. Gautam, S. Vanga, F. Ariese, S. Umapathy, EPJ Techn. Instrum. 2 (2015) 1.
[16] T. Naes, T. Isaksson, T. Fearm, T. Davies, A User-friendly Guide to Multivariate Calibration and Classification, NIR Publications, Chichester UK, 2002.
[17] S. De Vries, J.F. Cajo, C. Ter Braak, Chemom. Intell. Lab. Syst. 30 (1995) 239.
[18] K. Faber, B.R. Kowalski, Chemom. Intell. Lab. Syst. 34 (1996) 283.
[19] CAMO Software AS, The unscrambler appendices: method references, http://www.camo.com/helpdocs/The_Unscrambler_Method_References.pdf (Retrieved 17.10.2017).
[20] A.C. Olivieri, N.M. Faber, J. Ferre, R. Boque, J.H. Kalivas, H. Mark, Pure Appl. Chem. 78 (2006) 633.
[21] Y. Zhang, Quantification of Prediction Uncertainty for Principal Components Regression and Partial Least Squares Regression(Doctoral Thesis) University College London, 2014.
[22] J.N. Miller, J.C. Miller, Statistics and Chemometrics for Analytical Chemistry, 6th edition Pearson Education Limited, Essex UK, 2010 121–123.
[23] F. Westad, F. Marini, Anal. Chim. Acta 893 (2015) 14.
[24] K.D. Brown, G.A. Parker, Analyst 105 (1980) 1208.
[25] B.M. Wise, R.T. Roginski, IFAC-PapersOnLine 48 (2015) 260.
[26] R.N. Feudale, N.A. Woody, H. Tan, A.J. Myles, S.D. Brown, J. Ferré, Chemometr. Intell. Lab. 64 (2002) 181.